LAWRENCE
LIVERMORE
NATIONAL
LABORATORY

UCRL-JRNL-202570

Note Hyperviscosity for Shock-Turbulence Interactions

A. W. Cook, W. H. Cabot

February 26, 2004

Journal of Computational Physics

Note

Hyperviscosity for Shock-Turbulence Interactions

Andrew W. Cook and William H. Cabot

Lawrence Livermore National Laboratory, Livermore CA 94550

Key words: artificial viscosity, subgrid-scale model, shock-capturing, turbulence

PACS: 47.11.+j

Over half a century ago, von Neumann and Richtmyer [1] introduced the idea of adding artificial viscosity to the Euler equations in order to help stabilize shock calculations. Their ideas regarding artificial viscosity influenced Smagorinsky [2, 3] in his development of a subgrid-scale model designed to match the Kolmogorov spectrum for atmospheric turbulence (C. E. Leith, private communication). Since that time, numerous artificial viscosity formulations have been proposed for simulating both shocks and turbulence [4, 5, 6, 7, 8, 9, 10]. Over the years however, a rift has developed between shock-capturing (monotonicity-preserving) and turbulence-capturing (large-eddy simulation) methods. Artificial viscosities for shock-capturing typically depend on sound speed, which makes them unsuitable for low Mach number flows. On the other hand, subgrid-scale models, customized for incompressible turbulence, usually fail to capture shocks in a monotonic fashion. The purpose of this paper is to introduce an artificial viscosity suitable for computing

shock-turbulence interactions. This is accomplished by extending the model of Cook and Cabot [10] to multi-dimensions.

The Navier-Stokes equations for compressible flow of an ideal gas, with constant specific heats, are (underline denotes tensor):

$$\dot{\rho} + \nabla \cdot \rho \mathbf{u} = 0 \ , \tag{1}$$

$$\dot{\mathbf{m}} + \nabla \cdot (\rho \mathbf{u}\mathbf{u} + p\underline{\boldsymbol{\delta}} - \underline{\boldsymbol{\tau}}) = 0 \ , \tag{2}$$

$$\dot{E} + \nabla \cdot [E\mathbf{u} + (p\underline{\boldsymbol{\delta}} - \underline{\boldsymbol{\tau}}) \cdot \mathbf{u} + \mathbf{q}] = 0 \ , \tag{3}$$

$$p = (\gamma - 1)\rho e \ , \tag{4}$$

where ρ is density, $\mathbf{u}$ is velocity, $\mathbf{m} = \rho\mathbf{u}$ is momentum p is pressure, $\underline{\boldsymbol{\delta}}$ is the unit tensor, $E = \rho(e + \mathbf{u} \cdot \mathbf{u}/2)$ is total energy, e is internal energy and $\gamma = c_p/c_v$ is the ratio of specific heats. The viscous stress tensor, $\underline{\boldsymbol{\tau}}$, is given by

$$\underline{\boldsymbol{\tau}} = \mu(2\underline{\mathbf{S}}) + (\beta - \frac{2}{3}\mu)(\nabla \cdot \mathbf{u})\underline{\boldsymbol{\delta}} \ , \tag{5}$$

where μ is dynamic (shear) viscosity, β is bulk viscosity and $\underline{\mathbf{S}}$ is the symmetric strain rate tensor

$$\underline{\mathbf{S}} = \frac{1}{2}(\nabla\mathbf{u} + \mathbf{u}\nabla) \ , \tag{6}$$

where $\mathbf{u}\nabla$ denotes the transpose of $\nabla\mathbf{u}$. The conductive heat flux vector, $\mathbf{q}$, is given by Fourier's law, i.e.,

$$\mathbf{q} = -\sigma\nabla T \ , \tag{7}$$

where σ is thermal conductivity and $T = (\gamma - 1)e/R$ is temperature (with $R = c_p - c_v$ being the gas constant). At high Mach numbers and high Reynolds numbers, the Navier-Stokes equations admit scales of motion too small to practically resolve on numerical grids. A key problem in simulating such flows is how to properly remove energy above the Nyquist wavenumber without corrupting the remaining flow. We will demonstrate how an artificial viscosity with spectral-like behavior can accomplish this objective.

Our approach is to add grid-dependent components to the viscosity coefficients, i.e., $\mu = \mu_f + \mu_\Delta$ and $\beta = \beta_f + \beta_\Delta$ are used in (5), where the f subscript denotes physical viscosity and the Δ subscript denotes artificial viscosity. Spectral-like models for μ_Δ and β_Δ are

$$\begin{aligned} \mu_\Delta &= C_\mu^r \eta^r \\ &\quad , \quad \eta^r = \rho \Delta^{(r+2)} \overline{|\nabla^r S|} \ , \quad r = 2, 4, 6... \\ \beta_\Delta &= C_\beta^r \eta^r \end{aligned} \tag{8}$$

where Δ is local grid spacing and $S = (\underline{\mathbf{S}} : \underline{\mathbf{S}})^{1/2}$ is the magnitude of the strain rate tensor. The $\nabla^r S$ term denotes successive applications of the Laplacian operator, e.g., $r = 4$ corresponds to the biharmonic operator, $\nabla^4 S = \nabla^2(\nabla^2 S)$. The overbar ($\overline{\psi}$) denotes a truncated-Gaussian filter, defined as

$$\overline{\psi}(\mathbf{x}) = \int_{-L}^{L} G(||\mathbf{x} - \boldsymbol{\xi}||; L) \psi(\boldsymbol{\xi}) d^3\xi \ , \tag{9}$$

where

$$G(\zeta; L) = \frac{e^{-6\zeta^2/L^2}}{\int_{-L}^{L} e^{-6\zeta^2/L^2} d\zeta} \ , \quad L = 4\Delta \ . \tag{10}$$

In practice, (9) is approximated by taking a weighted average among neigh-

boring grid points. This filter helps remove high wavenumbers introduced by the absolute value operator, which in turn, ensures that the viscosities are positive definite.

Equation (8) corresponds to Smagorinsky's model if r, C_β^r and L are all set to 0. Inclusion of the bulk viscosity term is the key to capturing shocks without destroying vorticity, i.e., β can be made large (to smooth shocks) without impacting small-scale turbulence in regions where $\nabla \cdot \mathbf{u} \approx 0$. Additionally, by setting $r > 0$ the viscosity keys directly on the ringing, rather than indirectly on gradients. This eliminates the need for adhoc limiters and switches to turn off β in special cases, e.g., expansion, isentropic compression, rigid rotation etc. [8]. It also removes the need for a "dynamic procedure" [11] to turn off μ in regions of uniform shear. The Laplacian operator(s) have some theoretical justification in that they impart a high-wavenumber bias to the artificial viscosity, thus approximating the cusp in the Heisenburg-Kraichnan spectral viscosity [12, 13] for isotropic turbulence. Cook and Cabot [10] have demonstrated, for smooth flow in 1 dimension, that higher convergence rates can be achieved by increasing r. However, larger values of r require higher-order approximations for the derivatives. Anticipating implementation of the model on nonuniform grids, where only a single Laplacian is feasible, we chose $r = 2$ for the current simulations and set $C_\mu^2 = 0.025$ and $C_\beta^2 = 5$. Recommended values for the empirical coefficients with $r = 4$ are $C_\mu^4 = 0.002$ and $C_\beta^4 = 1$.

In evaluating the model, it is desirable to use a numerical scheme with low truncation error and minimal implicit dissipation, which would otherwise compete with $\underline{\boldsymbol{\tau}}$. Therefore we use Fourier transforms to compute spatially-periodic derivatives, a tenth-order compact scheme [14] for nonperiodic derivatives, and a 4th-order Runge-Kutta (RK4) scheme for temporal integration. Dealiasing

is accomplished by applying a (2/3)-wavenumber truncation to the conserved variables after each RK4 substep. Details of the numerical method are given in Cook and Cabot [10]. The simulations reported here were all performed on uniform Cartesian grids, where $\Delta x = \Delta y = \Delta z = \Delta$.

Our first test case is a canonical model of a one-dimensional shock-turbulence interaction, i.e., Shu's problem [15]. The initial conditions are: $\rho = 3.857143$, $p = 10.33333$ and $u = 2.629369$ for $x < -4$; $\rho = 1 + 0.2\sin(\pi x)$, $p = 1$ and $u = 0$ for $x \geq -4$, and $\gamma = 1.4$. As the shock propagates into the sinusoidal density field, it leaves a steeply oscillating flow in the post-shock region. Figure 1 shows the effect of the hyperviscosity model on the flow, where "model off" corresponds to $C_\mu^r = C_\beta^r = 0$. The model removes nonphysical oscillations surrounding the shock without attenuating physical oscillations in the shock's wake.

Our second test case is the spherical Noh implosion [16]. The initial conditions are: $\rho = 1$, $p = 0$ and $\mathbf{u}$ = unit vector directed toward origin, with $\gamma = 5/3$. In this problem, an infinite-strength shock expands outward from the origin at a constant velocity of 1/3. This objective here is to test the ability of a scheme to preserve spherical symmetry and produce the correct entropy jump for adiabatic shock compression. In some sense, this problem represents a worst-case scenario for artificial viscosity methods, since any additional heating from the dissipation function results in reduced compression. This test case suffers a well-known "wall heating" problem [16, 8], arising from the singularity in the initial velocity field. Hence, for this problem only, we adopted the standard remedy of introducing an artificial thermal conductivity, namely $\sigma_\Delta = 5c_p\rho\Delta\sqrt{|e|}$. This has the effect of spreading out heat near the origin. In Fig. 2, density is plotted versus radius at two different angles to the grid.

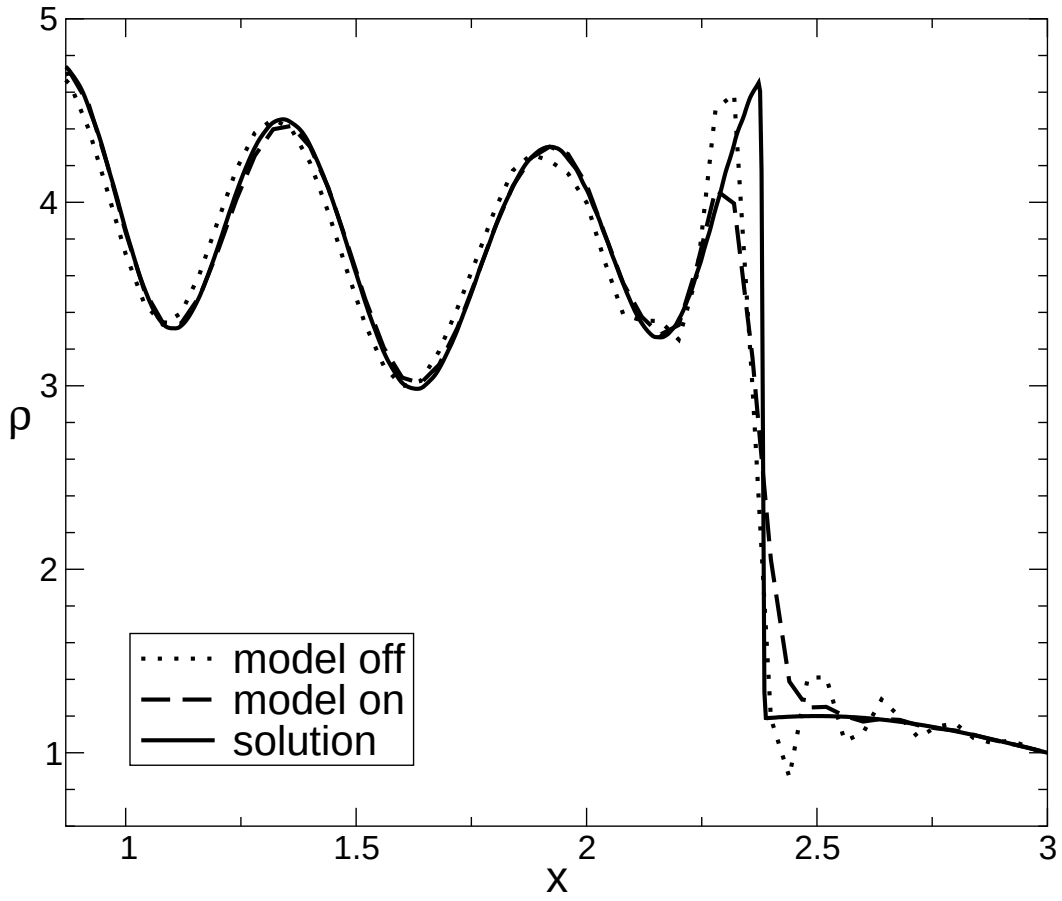

Fig. 1. Density field for Shu's problem at $t = 1.8$. The solid curve is the converged solution. The "model off" and "model on" simulations were both conducted at a grid resolution of $\Delta = 0.04$.

Without the hyperviscosity model, the simulation became unstable (with or without σ_Δ) and failed to complete; hence, only the results with the model active are shown. As indicated by the coincidence of the on-axis and off-axis density curves, the model is insensitive to grid orientation, i.e., it maintains spherical symmetry, albeit with a slight amount of post-shock ringing in grid-aligned directions (dotted line). Regarding the entropy jump, the simulated shock does not quite produce the theoretical post-shock density of $\rho = 64$ due to viscous heating. This however, is not much different than results produced

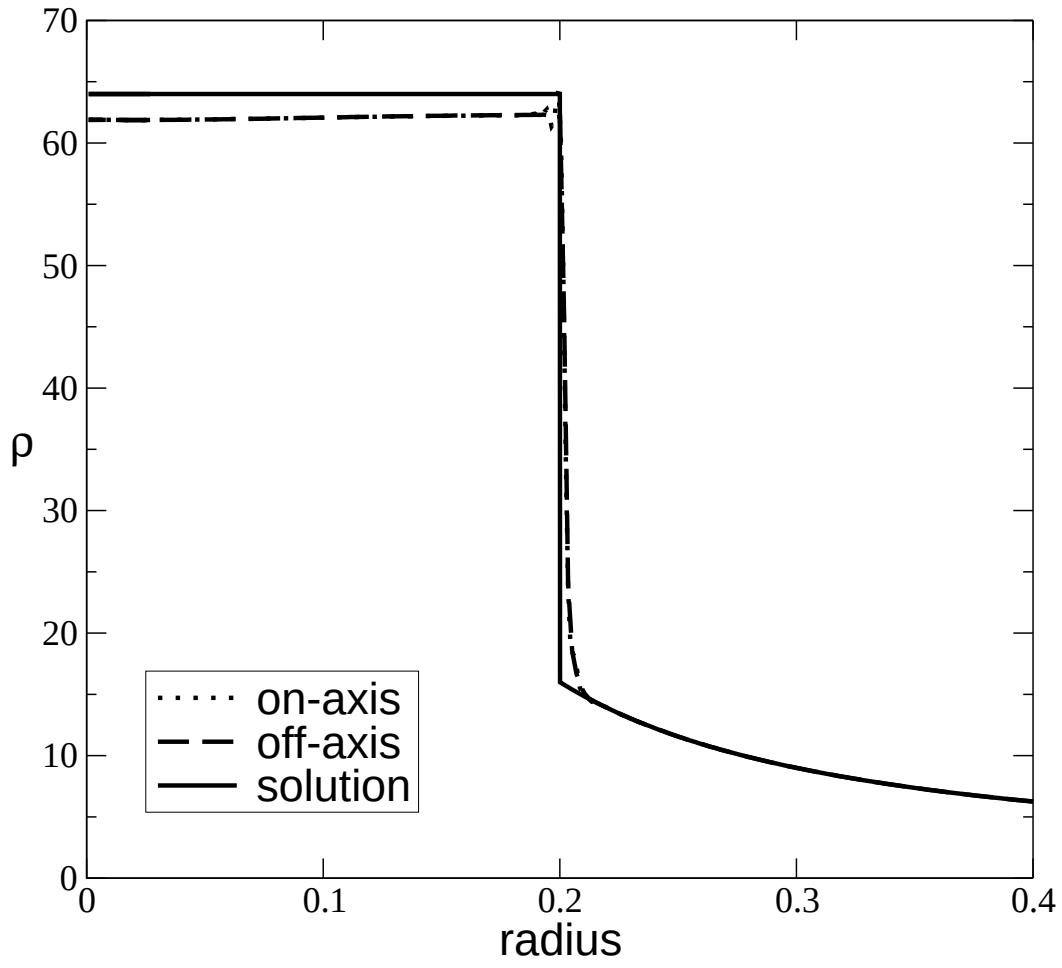

Fig. 2. Density versus radius for Noh's problem at $t = 0.6$. The dotted line is along the z-axis ($\theta = \phi = 0$) and the dashed line is diagonal to the grid ($\theta = \phi = 45^o$). The simulation was conducted on an octant of a sphere with $\Delta = 10^{-3}$.

by Arbitrary Lagrangian Eulerian (ALE) methods [8]. The compression ratio is resolution dependent; e.g., for $\Delta = 5 \times 10^{-3}$ and $\Delta = 10^{-3}$ the post-shock density is 55.2 and 62.3, respectively. Therefore, the artificial bulk viscosity method is applicable to very strong shocks, provided sufficient resolution is allocated to the problem.

Our third test case is the Taylor-Green vortex [17]. This problem is designed to

test a model's ability to preserve resolved-scale vorticity. The initial conditions are:

$$
\begin{aligned}
\rho &= 1 \\
u &= \sin(x)\cos(y)\cos(z) \\
v &= -\cos(x)\sin(y)\cos(z) \\
w &= 0 \\
p &= 100 + \rho\{[\cos(2z)+2][\cos(2x)+\cos(2y)]-2\}/16 \\
\gamma &= 1.4
\end{aligned}
$$

where the pressure corresponds to incompressible flow (Poisson solution). The arbitrary constant of 100 is selected to make the Mach number very low, such that the flow remains essentially incompressible. The flow domain (V) is a triply-periodic $(2\pi)^3$ box on a 64^3 grid. The vortex stretches and bends, driving vorticity to smaller scales. Figure 3 shows normalized total enstrophy, i.e., $\Omega(t)/\Omega(0)$, where

$$\Omega(t) = \frac{1}{2}\int_V \boldsymbol{\omega}\cdot\boldsymbol{\omega}\, dV \ , \quad \boldsymbol{\omega} = \nabla\times\mathbf{u} \ ,$$

as a function of time, for simulations with and without the model. The semi-analytic solution [18, 19], accurate up to about $t = 3.5$, is also plotted for comparison. The simulations give nearly identical results so long as the flow is well-resolved. It is only late in time, when vorticity begins to concentrate near the grid scale, that μ_Δ begins to damp velocity gradients.

Our fourth and final test case is the decaying turbulence experiment of Kang et al. [20]. In their experiment, air is blown past an active grid in the Corrsin wind tunnel [21, 22], generating near-isotropic turbulence at a Taylor microscale Reynolds number of about 720. An array of four X-wire probes is used to measure velocity at downstream stations: $x/M = 20,\ 30,\ 40$ & 48, where M is the shaft spacing of the active grid. The initial conditions for the

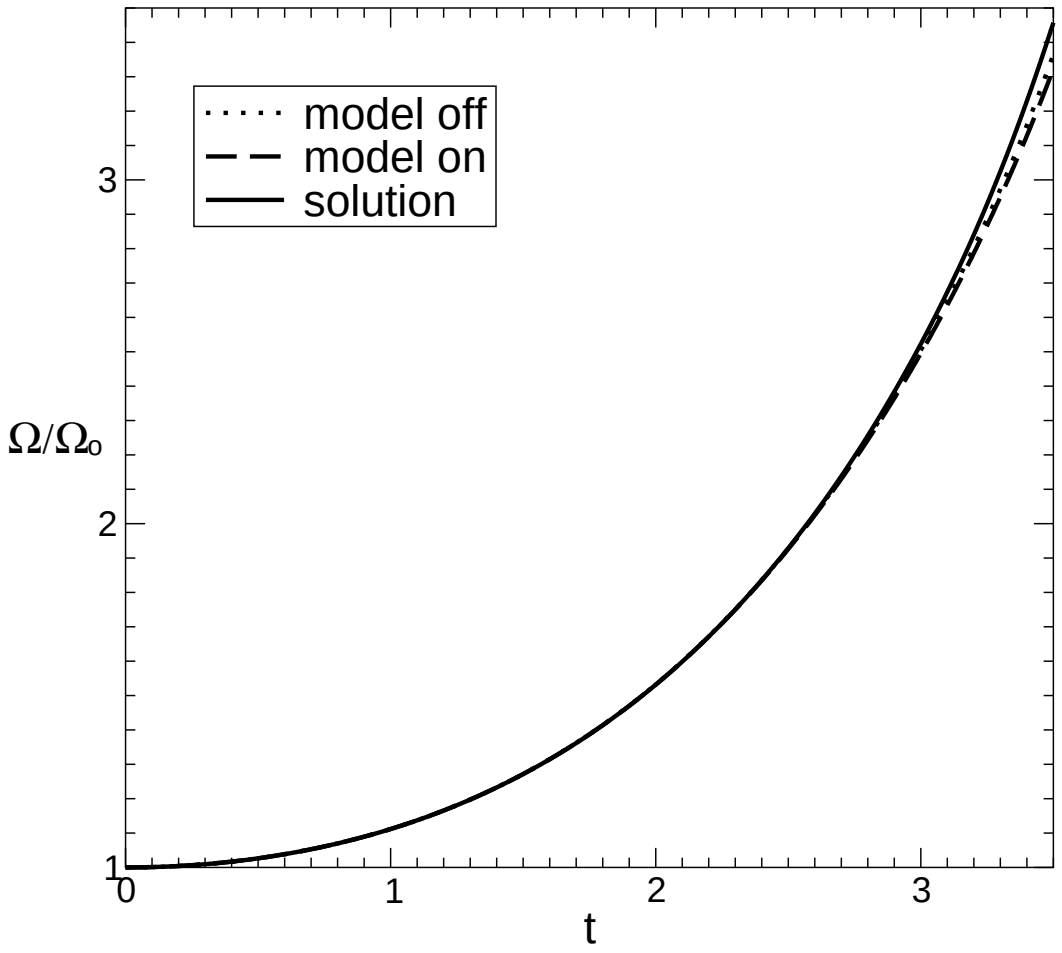

Fig. 3. Normalized enstrophy for the Taylor-Green vortex with $\Delta = 2\pi/64$.

simulations consist of a triply-periodic velocity field in a 192^3 box, with a kinetic energy spectrum matched to first 64 wavenumbers of the experimental spectrum at $x/M = 20$. Pressure is initialized by solving a Poisson equation with $\nabla \cdot u = 0$. Simulation time is related to distance downstream using the mean flow velocity, i.e., $x = Ut$. Figure 4 depicts the evolution of the 3-D kinetic energy spectrum, $E(k)$, as well as the decay of turbulent kinetic energy, KE, for the experiment and simulations. The results indicate that the hyperviscosity model provides the correct rate of subgrid-scale energy transfer, resulting in a robust Kolmogorov, $k^{(-5/3)}$, spectrum and correct rate of energy

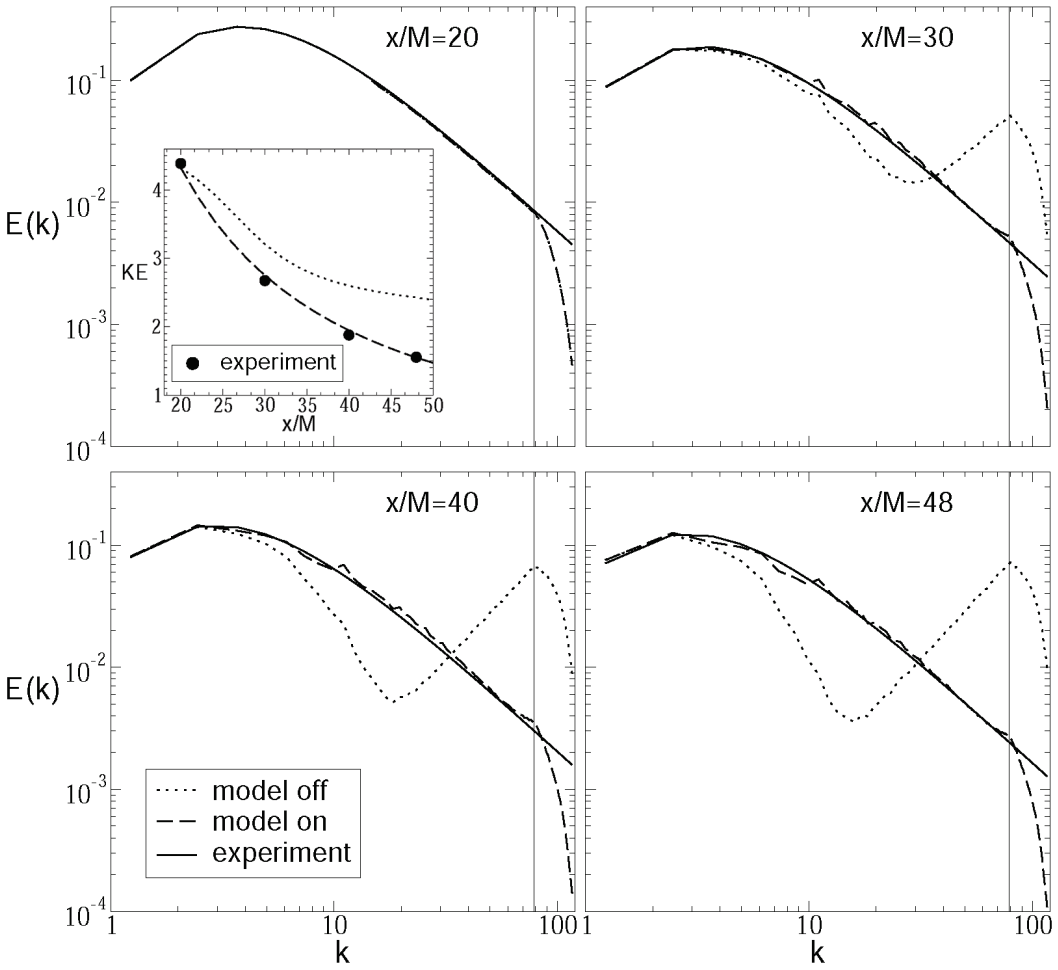

Fig. 4. Evolution of 3-D energy spectrum, E(k), for high Reynolds number wind tunnel experiment of Kang et al. [20]. The inset in the first plot shows decay of turbulent kinetic energy (KE). The vertical lines correspond to the 2/3 wavenumber truncation, which serves to dealias the numerical simulations.

decay. With no subgrid-scale model, the spectral energy flux is corrupted, as evidenced by the anomalous curvature of the spectrum and too-rapid decay of turbulent kinetic energy.

In summary, we have proposed an artificial viscosity suitable for both shocks and turbulence. It employs a bulk viscosity, designed to produce monotonic

shocks, and a dynamic viscosity, designed to model subgrid-scale turbulence. The model is straightforward to implement and should provide improved means for simulating shock-turbulence interactions.

Acknowledgements

We are grateful to Profs. A. Leonard, D. Pullin and P. Dimotakis for their advice regarding this effort. This work was performed under the auspices of the U.S. Department of Energy by the University of California Lawrence Livermore National Laboratory under contract No. W-7405-Eng-48.

References

[1] J. von Neumann and R. D. Richtmyer. A method for the numerical calculations of hydrodynamical shocks. *J. Appl. Phys.*, 21:232–237, 1950.

[2] J. Smagorinsky. General circulation experiments with the primitive equations, part i: The basic experiment. *Mon. Weather Rev.*, 91:99–152, 1963.

[3] J. Smagorinsky. *Some Historical Remarks on the Use of Nonlinear Viscosities*, pages 2–36. Cambridge University Press, 1993.

[4] A. Jameson, W. Schmidt, and E. Turkel. Numerical simulation of the euler equations by finite volume methods using runge-kutta time stepping schemes. AIAA paper 81-1259, AIAA 5th Computations Fluid Dynamics Conference, 1981.

[5] E. Tadmor. Convergence of spectral methods for nonlinear conservation laws. *SIAM J. Numer. Anal.*, 26:30, 1989.

[6] C. K. W. Tam, J. W. Webb, and Z. Dong. A study of the short wave components in computational aeroacoustics. *J. Comput. Acoustics*, 1: 1–30, 1993.

[7] A. Misra and D. I. Pullin. A vortex-based subgrid stress model for large-eddy simulation. *Phys. Fluids*, 9:2443–2454, 1997.

[8] E. J. Caramana, M. J. Shashkov, and P. P. Whalen. Formulations of artificial viscosity for multi-dimensional shock wave computations. *J. Comput. Phys.*, 144:70–97, 1998.

[9] G-S. Karamanos and G. E. Karniadakis. A spectral vanishing viscosity method for large-eddy simulations. *J. Comput. Phys.*, 163:22–50, 2000.

[10] A. W. Cook and W. H. Cabot. A high-wavenumber viscosity for high-resolution numerical methods. *J. Comput. Phys.*, ???:??–??, 2004.

[11] P. Moin, K. Squires, W. Cabot, and S. Lee. A dynamic subgrid-scale model for compressible turbulence and scalar transport. *Phys. Fluids*, 3: 2746–2757, 1991.

[12] W. Heisenburg. Zur statistischen theorie der turbulenz. *Z. Phys.*, 124: 628–657, 1948.

[13] R. H. Kraichnan. Eddy viscosity in two and three dimensions. *J. Atmos. Sci.*, 33:1521–1536, 1976.

[14] S. K. Lele. Compact finite difference schemes with spectral-like resolution. *J. Comput. Phys.*, 103:16–42, 1992.

[15] C.-W. Shu and S. J. Osher. Efficient implementation of essentially non-oscillatory shock capturing schemes ii. *J. Comput. Phys.*, 83:32–78, 1989.

[16] W. F. Noh. Errors for calculations of strong shocks using an artificial viscosity and an artificial heat flux. *J. Comput. Phys.*, 72:78–120, 1987.

[17] G. I. Taylor and A. E. Green. Mechanism of the production of small eddies from large ones. *Proc. Roy. Soc. A*, 158:499–521, 1937.

[18] R. H. Morf, S. A. Orszag, and U. Frisch. Spontaneous singularity in three-dimensional, inviscid, incompressible flow. *Phys. Rev. Lett.*, 44:572–575, 1980.

[19] M. E. Brachet, D. I. Meiron, S. A. Orszag, B. G. Nickel, R. H. Morf, and U. Frisch. Small-scale structure of the Taylor-Green vortex. *J. Fluid Mech.*, 130:411–452, 1983.

[20] H. S. Kang, S. Chester, and C. Meneveau. Decaying turbulence in an active-grid-generated flow and comparisons with large-eddy simulation. *J. Fluid Mech.*, 480:129–160, 2003.

[21] G. Comte-Bellot and S. Corrsin. The use of a contraction to improve the isotropy of grid-generated turbulence. *J. Fluid Mech.*, 25:657–682, 1966.

[22] G. Comte-Bellot and S. Corrsin. Simple eulerian time correlation of full and narrow-band velocity signals in grid-generated 'isotropic' turbulence. *J. Fluid Mech.*, 48:273–337, 1971.